Journal of Inorganic Biochemistry 117 (2012) 351–358

Contents lists available at SciVerse ScienceDirect

Journal of Inorganic Biochemistry

journal homepage: www.elsevier.com/locate/jinorgbio

Metal ions affect insulin-degrading enzyme activity

Giuseppe Grasso [a,*], Fabrizio Salomone [a,1], Grazia R. Tundo [b,c], Giuseppe Pappalardo [d], Chiara Ciaccio [b,c], Giuseppe Spoto [a,d,e], Adriana Pietropaolo [f], Massimo Coletta [b,c], Enrico Rizzarelli [a,d,e]

[a] Dipartimento di Scienze Chimiche, Università di Catania, Viale Andrea Doria 6, 95125 Catania, Italy
[b] Dipartimento di Scienze Cliniche e Medicina Traslazionale, Università di Roma Tor Vergata, Via Montpellier 1, I-00133 Roma, Italy
[c] Consorzio Interuniversitario di Ricerca in Chimica dei Metalli nei Sistemi Biologici, Via C. Ulpiani 27, I-70126 Bari, Italy
[d] Istituto Biostrutture e Bioimmagini, CNR, Viale A. Doria 6, 95125 Catania, Italy
[e] Consorzio I.N.B.B., Viale delle Medaglie d'Oro 305, 00136, Roma, Italy
[f] University of Catanzaro, Campus Universitario, Viale Europa, 88100 Catanzaro, Italy

ARTICLE INFO

Article history:
Received 22 March 2012
Received in revised form 7 June 2012
Accepted 10 June 2012
Available online 23 June 2012

Keywords:
Copper
Zinc
IDE
Insulysin
Kinetics
Metals

ABSTRACT

Insulin degradation is a finely tuned process that plays a major role in controlling insulin action and most evidence supports IDE (insulin-degrading enzyme) as the primary degradative agent. However, the biomolecular mechanisms involved in the interaction between IDE and its substrates are often obscure, rendering the specific enzyme activity quite difficult to target. On the other hand, biometals, such as copper, aluminum and zinc, have an important role in pathological conditions such as Alzheimer's disease or diabetes mellitus. The metabolic disorders connected with the latter lead to some metallostasis alterations in the human body and many studies point at a high level of interdependence between diabetes and several cations. We have previously reported (Grasso et al., Chem. Eur. J. 17 (2011) 2752–2762) that IDE activity toward Aβ peptides can be modulated by metal ions. Here, we have investigated the effects of different metal ions on the IDE proteolytic activity toward insulin as well as a designed peptide comprising a portion of the insulin B chain (B20–30), which has a very low affinity for metal ions. The results obtained by different experimental techniques clearly show that IDE is irreversibly inhibited by copper(I) but is still able to process its substrates when it is bound to copper(II).

1. Introduction

Insulin degradation plays a major role in controlling insulin activity and most evidence supports IDE (insulin-degrading enzyme) as the primary degradative agent [1,2]. IDE is a zinc metalloprotease containing an unusual inverse zinc-binding site, HxxEH, that is involved in catalysis [3]. Many in vitro and in vivo studies have shown that IDE is able to degrade several different substrates besides insulin [4], and amyloid-β peptides (Aβs) among the others [5]. For this reason, as hyperinsulinemia is associated with a high risk of Alzheimer's disease (AD) [6,7], IDE could play a critical role in the mechanism associating hyperinsulinemia and type 2 diabetes (DM2) with AD. Despite the evident role of IDE in various diseases, relatively little is known about its physiological functions and for this reason the control of its activity has been recently targeted as a viable approach in the study of diseases such as AD and insulin-dependent diabetes [8–10].

Since the discovery of insulin and Aβ cleavage by IDE [11], much effort has been put in trying to understand some key questions regarding cleavage sites [12,13], kinetics of substrate interaction [14,15] and the mechanism of IDE modulation [16,17].

It is often reported that the common feature shared by IDE substrates is the ability to form, under certain physiological conditions, amyloid fibrils [18–21]. Furthermore, several evidences indicate that the selective binding of IDE's substrates and their unfolding and processing are driven by the unique size, shape and electrostatic potential of the catalytic chamber and by interaction with the exosite [22,23]. However the molecular basis of the enzymatic activity modulation has only begun to be elucidated.

In this scenario, as metal ions are essential for many metabolic processes and their homeostasis is crucial for life [24–26], the elucidation of their roles on the modulation of IDE activity represents an important issue that could give an insight on the biomolecular mechanisms involved with the above mentioned diseases. Recently, zinc [27] and copper [28] have been identified to have a crucial role on insulin action and, ultimately, in diseases such as DM2. In particular, zinc deficiency seems to facilitate diabetes mellitus and its cardiovascular complications [29,30]. Although some studies have demonstrated antidiabetogenic properties of zinc supplementation in both animal models and humans, the efficacy is still controversial

* Corresponding author.
E-mail address: grassog@unict.it (G. Grasso).
[1] Current address: NEST — Center for Nanotechnology Innovation Piazza San Silvestro, 12, Pisa, Italy.

0162-0134/$ – see front matter © 2012 Elsevier Inc. All rights reserved.
doi:10.1016/j.jinorgbio.2012.06.010

and the observation that all patients could benefit from ion administration is too simplistic [31–34]. Interestingly, it has also been shown that copper chelating agents might be useful for the treatment of glucose and lipid dismetabolism in DM2 mouse model [28].

There are at least three different ways by which metal ions could, in principle, affect IDE proteolytic activity:

i. a change of conformation induced by metal ions on IDE substrates can produce proteolytic resistant species. In this respect, it has been reported that zinc, but not copper, induces the formation of Aβ aggregates resistant to IDE proteolytic action [35,36]. These data indicate that external factors, such as high metal concentrations that promote Aβ aggregate formation, may contribute to Aβ accumulation by decreasing the peptide's sensitivity to proteolytic degradation;
ii. direct binding of metal ions to IDE could alter the activity of the enzyme. Metal ions have long been recognized to stabilize and activate enzymes [37,38]. For several proteins, binding of metal cofactors, such as calcium, magnesium, manganese, copper, zinc and iron in different oxidation states, has been shown to increase the thermal stabilities of the proteins [39,40] and to substantially influence their structure and activity [41–43]. Modulation of the proteolytic activity of IDE could therefore occur through different routes such as coordination of exogenous ligands to the catalytic metal, substitution or removal of the latter [44–51]. Moreover, metals could bind either to residues present in the active site to block substrate interaction or to residues outside the active-site to affect the structural integrity of the enzyme [42,43];
iii. some metals could modulate the IDE expression and location in vivo.

However, the three above mentioned metal-driven alterations are often interconnected with difficulties in attributing a definite role to metal ions. For example, the investigation of the effect of divalent cations on insulin degradation by human erythrocyte fractions has produced different results if carried out by the membranous fractions or by all the erythrocyte fractions [52]. Analogously, in vitro investigation of the effect of metal ions on IDE capability to degrade insulin turned out to be difficult to interpret due to the combined action of metals both on the substrate and enzyme conformational features [53]. Therefore, the mechanisms of IDE activity modulation by metal ions remain elusive.

We have recently demonstrated that copper in different oxidation states is a strong inhibitor and zinc is a slight activator of IDE proteolytic activity toward Aβ peptides [54], being aware of the different metal complexes that the Aβ peptides form in solution and of their stability constants [55–57]. In this work, we investigate IDE activity on insulin and on a peptide substrate encompassing the 20–30 amino acid residues of the bovine insulin B chain (B20–30), which does not contain binding sites for metal ions, thus discriminating between the changes on peptide degradation brought about by the metal/enzyme interaction and the metal-driven alteration of the substrate conformation. Therefore, insulin as well as B20–30 digestions by IDE has been comparatively carried out in the presence and in the absence of copper(II), zinc(II), aluminum(III), copper(I) and silver(I), giving a clear picture of the effect of different metal ions on IDE activity.

2. Experimental

2.1. Materials

IDE, His-Tag, rat, recombinant, from *Spodoptera frugiperda* was purchased from Calbiochem and its activity was verified by carrying out enzymatic digestion of insulin solutions according to the experimental procedure previously reported [13]. In order to improve the reproducibility of the enzymatic assays carried out in the presence of metal ions, we have chosen to use the recombinant enzyme of a same commercial lot to minimize the differences on the absolute proteolytic activity of IDE found in the different commercial lots purchased (see Results and discussion section). It is also important to highlight that, although the recombinant enzyme used has been already tested as a good model for human IDE [13], the latter could, in principle, behave differently in the presence of metal ions. However, we have assumed that the His-Tag of the recombinant enzyme should not alter the IDE capability to bind metal ions because the concentration of the latter in the enzymatic assays are always at least about three orders of magnitude higher than the IDE concentration. In such experimental conditions, there are always free metal ions in solution and those bound to the His-Tag can be neglected.

Insulin from bovine pancreas (molecular mass = 5733.5 Da), phosphate-buffered saline (PBS), α-cyano-4-hydroxycinnamic acid (CHCA), trifluoroacetic acid (TFA) and acetonitrile (CH_3CN), Ac_2Cu, $KAl(SO_4)_2$, $AgNO_3$ and Ac_2Zn were all purchased from Sigma-Aldrich, while $ZipTip_{C18}$ pipette tips were from Millipore. High-purity water (Milli-Q Element Ultrapure Water) was used for preparation of all the solutions. All buffers and sample solutions were bubbled with argon to displace any dissolved air. All N-fluorenylmethoxycarbonyl (Fmoc)-protected amino acids, 2-(1-H-benzotriazole-1-yl)-1,1,3,3-tetramethyluronium tatrafluoroborate (TBTU) and polyethylene glycol-grafted polystyrene resin, bearing the Rink amide linker 4-[(2,4-dimethoxyphenyl)-aminomethyl]-phenoxyacetic acid (NovaSyn® Tenta Gel Rink, TGR) resin were obtained from Novabiochem (Switzerland); Fmoc-protected PAL-polyethylene glycol-grafted polystyrene resin (PAL–PEG; PAL = 5-(4-aminomethyl-3,5-dimethoxyphenoxy)valeric acid), N,N-diisopropylethylamine (DIEA) and N-[(dimethylamino)-1H-1,2,3-triazolo[4,5-b] pyridine-1-ylmethylene]-N-methylmethanaminium hexafluorophosphate N-oxide (HATU) were obtained from Applied Biosystems. N-hydro xybenzotriazole (HOBt), triisopropylsilane (TIS) and piperidine (Biotech grade) were purchased from Sigma-Aldrich. N,N-dimethylformamide (DMF, peptide synthesis grade) was obtained from Labscan Analytical Sciences. All other chemicals were of the highest available grade and were used without further purification.

Preparative reversed-phase (RP-) HPLC was carried out using a Varian PrepStar 200 model SD-1 chromatography system equipped with a Prostar photodiode array detector with detection at 222 nm. Purification was carried out by eluting with solvents A (0.1% TFA in water) and B (0.1% TFA in acetonitrile) on a Varian Microsorb 300 C18 250 × 41.4 mm (300 Å pore size, 10 μm particle size) column, at a flow rate of 30 ml/min. Analytical RP-HPLC analyses were performed using a Waters 1525 instrument equipped with a Waters 2996 photodiode array detector with detection at 222 nm. The peptide samples were analyzed using gradient elution with solvents A and B on a Vydac C18 250 × 4.6 mm (300 Å pore size, 5 μm particle size), run at a flow rate of 1 ml/min.

2.2. Peptide synthesis and purification

AcGlyGluArgGlyPhePheTyrThrProLysAlaNH$_2$ (B20–30) peptide was synthesized by using a microwave-assisted solid phase-peptide synthesis technology on a Liberty Peptide Synthesizer. Amino acid derivatives were introduced according to the TBTU/HOBt/DIEA method on a NovaSyn TGR resin (substitution 0.18 mmol/g).

All the coupling reactions were carried out under a 4-fold excess of amino acid at every cycle. The following instrumental conditions were used for each coupling cycle: microwave power of 30 W, reaction temperature of 75 °C, and coupling time of 300 s. Fmoc deprotection was achieved at every cycle with 20% piperidine solution in DMF, using the instrumental conditions: microwave power of 30 W, reaction temperature of 75 °C, and deprotection time of

180 s. N-terminal acetylation of B20–30 was performed by treating the fully assembled and protected peptide resin (after removal of the N-terminal Fmoc group) with a solution containing acetic anhydride (6% v/v) and DIEA (5% v/v) in DMF.

The peptide was cleaved from its resin and simultaneously deprotected by treatment with a mixture of TFA/TIS/H_2O (95/2.5/2.5 v/v) for 2 h at room temperature. Solution containing the free peptide was separated from the resin by filtration and concentrated in vacuo at 30 °C. The peptide was precipitated with cold freshly distilled diethyl ether. The precipitate was then filtered, dried under vacuum, redissolved in water and lyophilized. The crude peptide was purified by preparative RP-HPLC, using the following instrumental conditions: from 0 to 15 min of isocratic elution in 10% of B, then linear gradient from 10% to 25% B in 15 min, finally isocratic elution in 25% B from 30 to 48 min [R_t = 41.0 min]. For analytical RP-HPLC: from 0 to 5 min of isocratic elution in 10% B, then linear gradient from 10 to 25% B in 15 min, finally isocratic elution in 25% B from 20 to 25 min [R_t = 22.8 min]. Electrospray ionization/mass spectrometry (ESI/MS) [Obsd *m/z*: $(M+H)^+$ 1313.6, $(M+2H)^{2+}$ 657.3 (see Fig. 1). Calculated *m/z* for $C_{62}H_{88}N_{16}O_{16}$ (monoisotopic) = 1312.7].

2.3. MS measurements

ESI/MS measurements were carried out by using a Finnigan LCQ DECA XP PLUS ion trap spectrometer operating in the positive ion mode and equipped with an orthogonal ESI source (Thermo Electron Corporation, USA). Sample solutions were injected into the ion source at a flow-rate of 5 μl/min, using nitrogen as the drying gas. The mass spectrometer was operated with a capillary voltage of 46 V and a capillary temperature of 200 °C, while the spray voltage was set at 4.3 kV.

Atmospheric pressure-matrix assisted laser desorption ionization (AP-MALDI)/MS measurements were carried out on the same spectrometer which was fitted with a MassTech Inc. (USA) AP-MALDI source. The latter consists of a flange containing a computer-controlled X–Y positioning stage and a digital camera, and is powered by a control unit that includes a pulsed nitrogen laser (wavelength of 337 nm, pulse width of 4 ns, pulse energy of 300 μJ, repetition rate of up to 10 Hz) and a pulsed dynamic focusing (PDF) module that imposes a delay of 25 μs between the laser pulse and the application of the high voltage to the AP-MALDI target plate. Laser power was attenuated to about 65%. The target plate voltage was 1.8 kV. The ion trap inlet capillary temperature was set at 210 °C. Capillary and tube lens offset voltages of 30 and 15 V, respectively, were applied. Other mass spectrometer parameters were as follows: multipole 1 offset at −3.75 V, multipole 2 offset at −9.50 V, multipole RF amplitude at 400 V, lens at −24.0 V and entrance lens at −88.0 V. Xcalibur software was used for the elaboration of mass spectra.

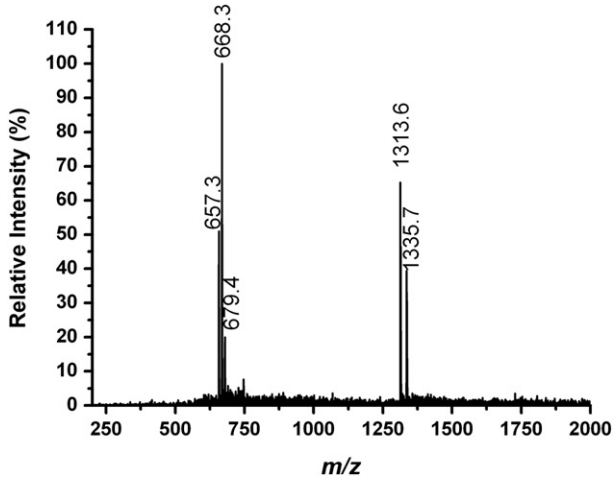

Fig. 1. ESI mass spectrum of the purified B20–30 peptide. The observed mass peaks are at the following *m/z* values: $(M+H)^+$ 1313.6, $(M+2H)^{2+}$ 657.3. Mono- and double-sodium adduct peaks are also detected.

Bovine insulin (molecular weight = 5733.5 Da) was used for mass calibration.

Enzymatic assays were carried out by preparing insulin or B20–30 solutions containing IDE and various metal ions in PBS buffer (150 mM) at various peptide/metal concentration ratios. All solutions, after a specific period of incubation at 37 °C, were desalted and concentrated by using ZipTips$_{C18}$. One drop of the purified solution was either diluted with 100 μl of water and injected into the ESI source or spotted on the target plate and, when dried, covered by a drop of the matrix solution (CHCA = 5 mM) in 30% of TFA (0.1%) and 70% of CH_3CN.

For the experiments with metal ions, aqueous solutions of Ac_2Cu, $KAl(SO_4)_2$, $AgNO_3$ or Ac_2Zn were added to the aliquoted peptide solutions to obtain the desired concentration of metal. In order to study the effect of copper(I) on IDE enzymatic activity, an excess of ascorbic acid [58] (Sigma) was added to an anaerobic reaction solution with $[Cu(I)(MeCN)_4](ClO_4)$ [59]. The latter was synthesized as follows: 50 ml of CH_3CN in a 100 ml Erlenmeyer flask was added with $Cu(II)(ClO_4)\cdot 6H_2O$ (2.5 g). An excess of powdered metallic copper (1.9 g) was then added and the reaction mixture was stirred for 4 h at room temperature. The solution was then filtered using a medium porosity frit, and the filtrate was concentrated by vacuum to ~20 ml. Diethyl ether (~25 ml) was then added slowly to the filtrate, and the solution was cooled overnight to yield white needle crystals of $[Cu(I)(MeCN)_4](ClO_4)$ that were used as the source of copper(I) ion in the enzymatic assay.

Because of the isotopic composition, molecular species are detected in the mass spectra as clusters of peaks; to simplify their assignments, the reported calculated values refer to monoisotopic *m/z*.

2.4. HPLC analysis of B20–30 hydrolysis by IDE

B(20–30) peptide was dissolved in 0.5 mM phosphate buffer at pH 7.3 and the peptide concentration was determined using an extinction coefficient of 1273 $cm^{-1}\,M^{-1}$ at 280 nm. Freshly dissolved peptide was incubated at 37 °C for 5 h with 10 nM IDE in 0.5 mM phosphate buffer, pH 7.3, in the presence or the absence of 100 μM copper(II), 100 μM silver(I), and 100 μM zinc(I). Metals have been previously incubated with IDE at 37 °C for 15 min before substrate addition. Aliquots were taken at different time intervals (i.e., 0 h, 15 min, 30 min, 1 h, 3 h, 5 h) and the reactions were stopped by addition of 0.5 mM EDTA. Samples were applied to a C18 reverse-phase HPLC column (Surveyor, Thermo Finnigan) and eluted at a flow rate of 1 ml/min using a linear gradient from 95% eluent A (H_2O + 0.1% TFA) and 5% eluent B (CH_3CN + 0.1% TFA) to 95% eluent B and 5% eluent A over a period of 65 min. The absorbance was monitored at 214, 222 and 280 nm.

Data have been analyzed by the double-reciprocal plot of velocity vs. the substrate concentration according to Eq. (1)

$$\frac{E_0}{v} = \frac{K_m}{k_{cat}\cdot[S]} + \frac{1}{k_{cat}} \quad (1)$$

where E_0 is the total enzyme concentration, v is the observed velocity (expressed as M/s), K_m is the Michaelis–Menten equilibrium constant (roughly corresponding to the substrate dissociation equilibrium constant), k_{cat} is the rate-limiting step velocity (expressed as s^{-1}) and [S] is the substrate concentration.

If metal binds only with the enzyme its modulatory effect on IDE activity shows the features of a non-competitive regulation and it may be described according to Scheme 1. In the latter, the interaction factor α represents the effect of metal binding on substrate binding (and vice versa): a value of $\alpha<1$ indicates a positive interaction, in

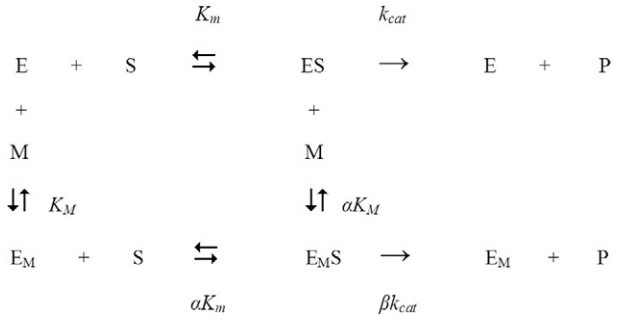

Scheme 1. Regulatory effect of a metal on IDE activity in the case of the metal binding only to the enzyme. K_M is the dissociation equilibrium constant of the metal ion (either silver(I), zinc(I) or copper(II)) to the free enzyme, α and β are interaction factors of the substrate affinity (in the case of α) and of the cleavage rate-limiting step (in the case of β), respectively, in the presence of metal.

which metal binding facilitates substrate binding (and vice versa); a value of $\alpha > 1$ represents a negative interaction; $\alpha = 1$ means no interaction between the two binding events. Different considerations can be made for the interaction factor β of the rate-limiting step k_{cat}: a value of $\beta > 1$ indicates that the substrate cleavage rate is enhanced when metal is bound to the enzyme; $\beta < 1$ means that the cleavage rate is slowed in the metal-bound enzyme; $\beta = 1$ refers to a lack of an effect by the metal on the substrate cleavage rate.

As from Scheme 1, the effect of the metal on two elements of Eq. (1) can be analyzed separately according to the following equations

$$\frac{K_m^{obs}}{k_{cat}^{obs}} = \frac{\alpha \cdot K_m \cdot (K_M + [M])}{k_{cat} \cdot (\alpha \cdot K_M + \beta \cdot [M])} \tag{2a}$$

$$\frac{1}{k_{cat}^{obs}} = \frac{\alpha \cdot K_m + [M]}{k_{cat} \cdot (\alpha \cdot K_m + \beta \cdot [M])} \tag{2b}$$

in which K_m^{obs} and k_{cat}^{obs} are the observed Michaelis–Menten equilibrium constant and the substrate cleavage rate-limiting step velocity, respectively, at a given metal concentration $[M]$, K_m and k_{cat} are the same parameters in the absence of the metal, K_M, α and β have the same meaning as described for Scheme 1. It must be pointed out that while parameters K_m, k_{cat}, α and β may vary with different substrates, the parameter K_M cannot, since it refers to the metal binding affinity to the free enzyme, independent on the interacting substrate.

2.5. Docking simulations

The starting coordinates of B20–30 were taken from the X-ray structure of human insulin (PDB code 3I3Z) [60]. The complex between IDE and the 1–18 portion of the B chain of insulin (PDB code 2WBY) [23] was used for the alignment of B20–30 prior to docking to IDE. The mutation E111Q present in 2WBY was replaced with E111. Docking simulations have been performed using the Haddock interface [61]. All residues of B20–30 were included as active residues for the Haddock docking, as well as Tyr831 and Arg824 of the IDE monomer. The zinc coordination site (Zn, His108, His112, Glu189, and Glu111) was kept fixed. Structures underwent rigid body energy minimization, and semirigid simulated annealing in torsion angle space, with a final clusterization of the results.

3. Results and discussion

3.1. Mass spectrometry studies of IDE proteolytic activity versus insulin peptides

Metal-induced insulin oligomerization is an important and widely investigated issue and several studies dealing with the effect of metal ions on insulin conformation have already been published [62]. Indeed, information regarding IDE enzymatic digestions of the full length insulin in the presence of metal ions is very problematic due to insulin aggregation and to the different peptide conformations existing at different peptide/metal ratios [63,64]. As a matter of fact, the ESI/MS characterization of samples containing insulin and metal ions reveals the presence of an insulin–metal interaction, as it is shown in Fig. 2, where the mass spectra obtained from the solutions that underwent IDE enzymatic digestion in the absence (Fig. 2a) and in the presence (Fig. 2b) of silver(I) are reported. The spectrum in Fig. 2b turns out to be unaltered before and after IDE enzymatic digestion, demonstrating the dramatic inhibitory role of silver(I) on IDE. The same mass spectrum was obtained when the insulin and metal addition order was inverted (i.e. IDE was preincubated with the metal). The same result was also obtained with copper(I). Both metal ions also partially disrupt insulin disulfide bridges as peaks attributed to insulin species that had lost a $-SH_2$ group are detected. A peak attributed to the insulin A chain also appears in the spectrum and is not recorded for insulin free solutions (data not shown). It is possible to see that while free insulin is normally degraded by IDE and the expected proteolytic fragments are detected, the insulin/silver complex is completely protease-resistant. However, the latter result could be explained in two different ways. Indeed, the total inhibition of IDE by the silver(I) ion could be attributed to the metal capability to bind and to inactivate the enzyme, but it could be as well possible that IDE is simply not able to degrade the silver–insulin complex that somehow could have a different conformation and/or oligomerization state from the free insulin (in Fig. 2b a peak assigned to the Ag/insulin$_2$ complex is also detected).

Therefore, in order to distinguish between the two above mentioned explanations, we have tested the effect of metal ions on IDE activity by using the B20–30 peptide. The latter has been designed to contain aminoacidic residues that do not form stable complexes with metal ions [65] and indeed it was not possible to detect any metal–peptide complex by AP-MALDI/MS experiments (see Fig. 3). Another advantage provided by the use of this peptide is that, because of its low molecular weight, it is possible to easily detect mono-charged species and so to carry out AP-MALDI/MS experiments instead of ESI/MS ones, whereas for insulin the high molecular weight

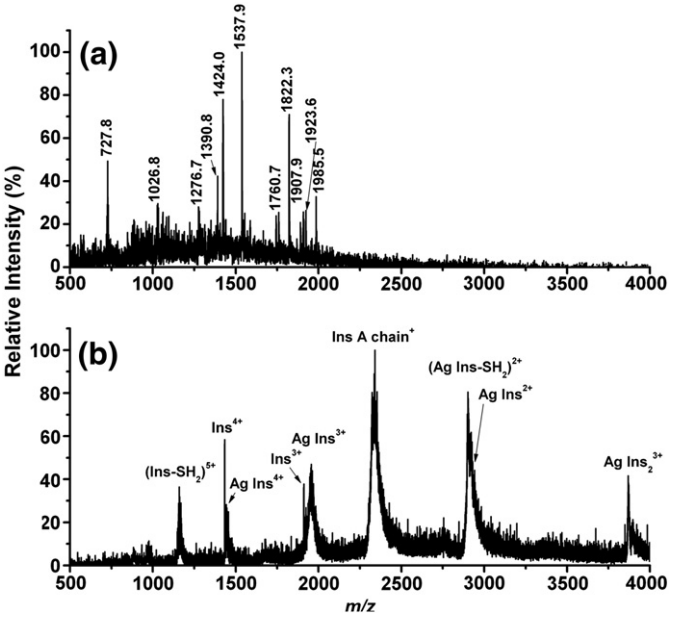

Fig. 2. ESI/MS results of the digestion of 18 μM insulin by IDE of 3.6 nM after 24 h of incubation at 37 °C in the absence (a) or in the presence (b) of 18 μM $AgNO_3$. A detailed assignment of the insulin proteolytic fragments reported in (a) can be obtained from Ref. [13].

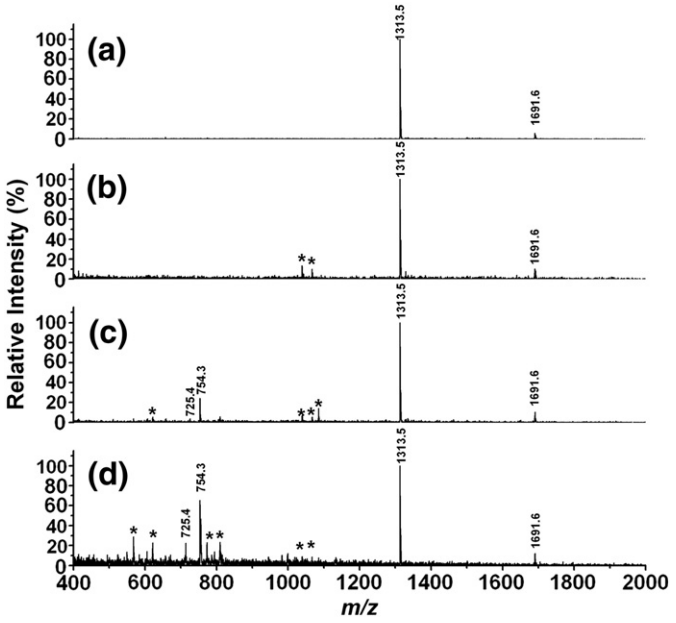

Fig. 3. AP-MALDI/MS results for the B20–30 peptide solution (1 μM) with 100 μM copper(II) that is (a) freshly prepared and (b) 1 week aged at 37 °C. The digestion of B20–30 by IDE of 3.6 nM at different periods of incubation, 1 h (c) and 24 h (d), are also reported. Fragments due to non-specific cleavage sites are indicated with an asterisk, while the complete assignment of the fragments is reported in Table 1. Peak at *m/z* 1691.6 is attributed to the adduct formed by the peptide with two matrix molecules, as confirmed by MS/MS experiments (data not shown).

hinders such an investigation (ion trap detection is in the range of *m/z* 0–4000). In this way, the mass spectra are simplified, while the screening of the different metal ions is faster and can be subjected to automation. We carried out enzymatic digestions of B20–30, in the presence or absence of copper(II), aluminum(III) and zinc(II), metals chosen for their important role in neurodegenerative diseases [24,26,66,67]. Moreover, since copper enters the cell as copper(I) through high-affinity plasma membrane copper transporters or low affinity permeases [68] and IDE is mainly cytosolic [1], it is interesting to analyze the effect of both oxidation states on B(20–30) processing. Furthermore, as silver belongs to the same group of copper and silver(I) has the same chemistry of copper(I), we have also performed studies using this ion, in order to have a replication of the copper(I) results without any possible invalidation due to copper(I) oxidation problems (although we worked in a reducing environment, copper(I) could be oxidized to copper(II) during the incubation with the enzyme).

In Fig. 3a the AP-MALDI/MS characterization of the newly synthesized B20–30 peptide is reported with copper(II) of 100 μM at time 0 h. It is possible to note from Fig. 3a and b that the B20–30 peptide does not undergo appreciable autolysis or fibrillation in the presence of the copper(II) ion neither immediately after the addition (see Fig. 3a) nor after 1 week of incubation at 37 °C (see Fig. 3b, where the molecular peak is still well visible in the spectrum). The mass spectra obtained from the digestion of B20–30 by IDE of 3.6 nM at different periods of incubation are also reported in Fig. 3c and d, while the cleavage sites of IDE inferred by the detected peptide fragments are depicted in Fig. 4. The principal fragments (see Table 1) are B20–25 (*m/z*: 754.3) and B26–30 (*m/z*: 725.4), indicating that two of the principal insulin cleavage sites (namely B(25–26) and B(24–25)) are specific cleavage sites for the interaction between IDE and insulin [13]. Other less specific peptide fragments also appear in the spectrum for a very long incubation time (Fig. 3d and Table 1 for the assignment).

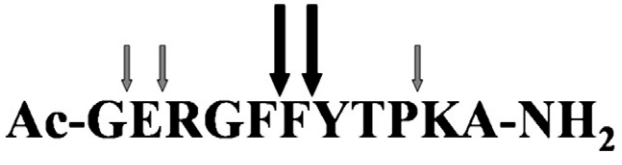

Fig. 4. Amino acid sequence of the synthesized B20–30 peptide tested for IDE activity assays. Big arrows indicate specific IDE cleavage sites while the small ones are indicative of other non-specific cleavages that are less favorable and mainly occur at a very long incubation time (≥24 h), possibly due to peptide autolysis (see Fig. 3b).

In Fig. 5 the AP-MALDI/MS results for the digestion of B20–30 by IDE in the presence or absence of the different metal ions are also reported and can be compared. Indeed, while aluminum(III) does not seem to affect the IDE proteolytic activity (Fig. 5a and d), the mass spectrum detected in the presence of copper(II) (Fig. 5c) clearly indicates a strong inhibition by copper(II) on the IDE enzymatic activity, since the spectrum is closely similar to that observed in the absence of the enzyme (Fig. 3a). Conversely, the intensities of peaks attributed to the intact B20–30 peptide clearly decrease their intensity when zinc(II) is present in the digestion solution (Fig. 5b), suggesting that zinc(II) somewhat enhances the IDE proteolytic activity on B20–30.

3.2. Effect of metal ions on B(20–30) processing by IDE

To assess how metal ions affect the IDE enzymatic activity, steady state kinetics on the B(20–30) peptide in the presence and in the absence of the above mentioned ions were performed. Fig. 6 shows the Lineweaver–Burk plot for the enzymatic degradation of B20–30 by IDE; catalytic parameters are reported in Table 2. From these data it comes out that the degradation of B20–30 by IDE is much slower than what was reported for insulin [52], at the peptide/enzyme concentration ratios used. Both the shorter chain length of this peptide [69] and the fact that in full length insulin the cleavages at the end of the B chain occur only after the initial cleavages in the middle of insulin A and B chains [23] might be responsible for the observed slower degradation rate by IDE. On the other hand, catalytic parameters for the cleavage of the B20–30 peptide are quite similar to those observed for the enzymatic processing of $A\beta_{1-40}$ (which showed a three-fold slower k_{cat} and a three-fold higher affinity for substrate, see Ref. [54]). It is also interesting to outline that if we compare these parameters with those obtained for the amyloid peptides $A\beta_{1-16}$ and $A\beta_{16-28}$ several similarities and some differences emerge [54]. In particular, the overall proteolytic activity toward the main cleavage sites (i.e., Phe_{24}-Phe_{25} and Phe_{25}-Tyr_{26} for B20–30, Glu_3-Phe_4, His_{13}-His_{14} and His_{14}-Gln_{15} for $A\beta_{1-16}$, Val_{18}-Phe_{19}, Phe_{19}-Phe_{20} and Phe_{20}-Ala_{21} for $A\beta_{16-28}$) is somewhat higher in the case of the B20–30 peptide due to a slightly more efficient cleavage rate-limiting step (see Table 2), whereas the substrate affinity of B20–30 appears intermediate between that of $A\beta_{1-16}$ (which is almost two-folds higher) and that of $A\beta_{16-28}$ (which is somewhat lower).

Fig. 6 also shows the effect of 100 μM copper(II) and of 100 μM zinc(II) on the enzymatic processing of B20–30 by IDE. The double-

Table 1
Assignment for the peptide fragments detected in Figs. 3 and 5 due to the cleavage of the peptide B20–30 by the action of IDE (see Fig. 4 for the cleavage sites). Calculated peaks refer to monoisotopic protonated species.

B20–30 peptide fragments	Experimental (*m/z*)	Calculated (*m/z*)
20–30	1313.5	1313.7
22–30	1085.5	1085.6
22–30 − H_2O	1067.5	1067.6
21–28 − H + Na	1039.0	1038.5
24–30	872.3	872.5
20–25	754.3	754.3
25–30	725.4	725.4
20–24	607.0	607.3

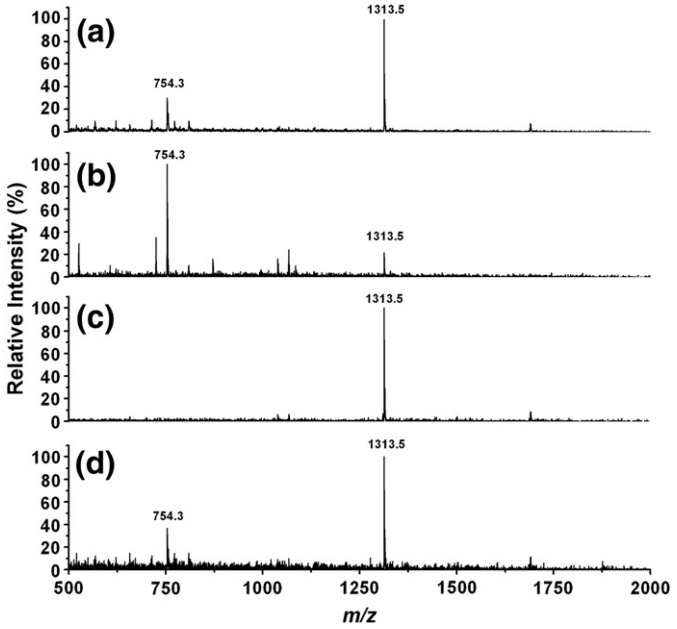

Fig. 5. AP-MALDI/MS results for the digestion of 1 μM B20–30 by IDE of 3.6 nM after a period of incubation of 24 h and in four different experimental conditions: (a) without metals, (b) with $[Zn^{2+}] = 100$ μM, (c) with $[Cu^{2+}] = 100$ μM and (d) with $[Al^{3+}] = 100$ μM. Discussion is in the text.

reciprocal plot for the enzymatic processing of B20–30 by IDE in the presence of 100 μM copper(II) shows a very marked inhibitory effect of copper(II) on the IDE proteolytic activity. This inhibition is even more significant in the case of silver(I) (which is employed instead of copper(I), due to the higher stability of the monovalent form under the experimental conditions), such that the enzyme is completely inactive toward the B20–30 peptide, similar to what has been observed in the case of the $A\beta_{16-28}$ peptide [54], and it is not reported in Fig. 6. On the other hand, the addition of 100 μM zinc(II) has a very modest effect, resulting in a two-fold increase of the overall

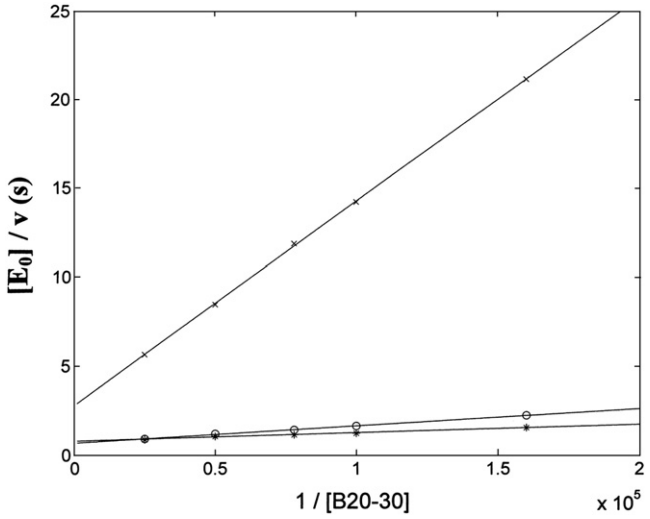

Fig. 6. Lineweaver–Burk plot of the enzymatic processing by IDE of (○) B(20–30) in the absence of metals; (x) B(20–30) in the presence of 100 μM copper(II); (*) B(20–30) in the presence of 100 μM zinc(II). Increasing concentrations of substrate were incubated with 10 nM IDE in 0.5 mM phosphate buffer at pH 7.3. Aliquots were taken at different time intervals (i.e., 0 h, 15 min, 30 min, 1 h, 3 h, 5 h) and samples were applied to a C18 reverse-phase HPLC column. A continuous line was obtained by a linear least-squares analysis according to Eq. (1). Catalytic parameters are reported in Table 2. In the presence of 100 μM silver(I) IDE enzymatic activity toward the B(20–30) peptide is abolished and data are not reported.

Table 2
Catalytic parameters for the enzymatic processing of the peptide B(20–30) by IDE and the effect of the addition of 100 μM copper(II) or of 100 μM zinc(II) at pH 7.3 and 37 °C.

	k_{cat}/K_m ($M^{-1}\,s^{-1}$)	k_{cat} (s^{-1})	K_m (M)
B_{20-30} peptide[a]	$1.03(\pm0.22)\times10^5$	1.47 ± 0.26	$1.43(\pm0.24)\times10^{-5}$
B_{20-30} + 100 μM Cu^{2+} [a]	$8.72(\pm1.14)\times10^3$	0.36 ± 0.05	$4.14(\pm0.63)\times10^{-5}$
B_{20-30} + 100 μM Zn^{2+} [a]	$2.09(\pm0.36)\times10^5$	1.26 ± 0.18	$6.03(\pm0.97)\times10^{-6}$
$A\beta_{1-40}$ [b]	$1.2(\pm0.2)\times105$	0.62 ± 0.08	$5.1(\pm0.7)\times10-6$
$A\beta_{1-16}$ [b]	$7.8(\pm0.9)\times10^4$	0.73 ± 0.09	$9.3(\pm1.6)\times10^{-6}$
$A\beta_{16-28}$ [b]	$5.9(\pm0.7)\times10^4$	1.18 ± 0.28	$2.0(\pm0.4)\times10^{-5}$
$A\beta_{1-16}$ + 100 μM Ag^{+} [b]	$1.7(\pm0.3)\times10^4$	0.094 ± 0.018	$5.5(\pm0.7)\times10^{-6}$
$A\beta_{16-28}$ + 100 μM Cu^{2+} [b]	$4.0(\pm0.6)\times10^4$	0.40 ± 0.06	$1.0(\pm0.3)\times10^{-5}$

[a] From this work.
[b] From Ref. [54].

enzymatic activity, fully referable to a higher substrate affinity (see Table 2).

Analysis of the copper(II) and zinc(II) effect according to Scheme 1 employing Eqs. (2a) and (2b) allows us to determine K_M for the two metals as well as the two interacting parameters α and β, which are reported in Table 3. It comes out that the two metals, which display a quite similar affinity for the binding site (as from the values of K_M, see Table 3), have opposite effects on the substrate affinity, since copper(II) binding brings about a three-fold decrease of the B20–30 affinity, whereas zinc(II) binding induces a two-fold increase of substrate affinity. Both metals lead to a reduction of the velocity for the rate-limiting step k_{cat} (as resulting from $\beta<1$, see Table 3), but the effect due to copper(II) binding is much more relevant than that referable to zinc(II) binding.

A very important aspect to be remarked is the fact that K_{Cu} ($=6.3(\pm2.1)\times10^{-6}$ M, see Table 3), resulting from the application of Scheme 1, is drastically different from the value reported before for the copper(II) effect on the enzymatic processing of $A\beta_{16-28}$ [54]. Since K_{Cu} referred to the interaction of copper(II) with free IDE, its value must be independent on the substrate. However, this discrepancy is simply due to the previous analysis [54], where we arbitrarily imposed $\beta=0$ (see Scheme 1 and Eqs. (2a) and (2b)), postulating that the E_MS species was completely inactive. This hypothesis is clearly incompatible with the copper(II) effect on the enzymatic processing of the peptide B20–30 by IDE, forcing us to employ a value of $\beta\neq0$. A new analysis of the copper(II) effect on the cleavage of $A\beta_{16-28}$ by IDE resulted in the following parameters (i.e., $K_{Cu}=6.3(\pm2.1)\times10^{-6}$ M, $\alpha=0.5\pm0.2$ and $\beta=0.32\pm0.05$), where the value of K_{Cu} was clearly imposed and the obtained α and β parameters can be compared with those obtained for the processing of B20–30.

The lowest energy docking structure of the complex between B20–30 and the IDE monomer (see Fig. 7) indicates that the active site for the protease activity faces the disordered segment ^{24}FFYT^{27}. A close proximity of T27 to the zinc(II) ion was identified with a distance of 2.3 Å. Threonine is so far deemed to orient the Zn–OH interaction, thereby reducing the activation barrier of the catalytic process, through a stabilization of the activation state via hydrogen bonds [70]. IDE catalysis starts through a nucleophilic attack to the carbonyl

Table 3
Dissociation equilibrium constant K_M for copper(II) and zinc(II) binding to IDE at pH 7.3 and 37 °C and interaction parameters α and β according to Scheme 1 and Eqs. (2a) and (2b).

	Copper(II)	Zinc(II)
K_M (M)	$6.3(\pm2.1)\times10^{-6}$	$1.0(\pm0.3)\times10^{-5}$
α	3.3 ± 0.5	0.4 ± 0.1
β	0.098 ± 0.024	0.86 ± 0.19

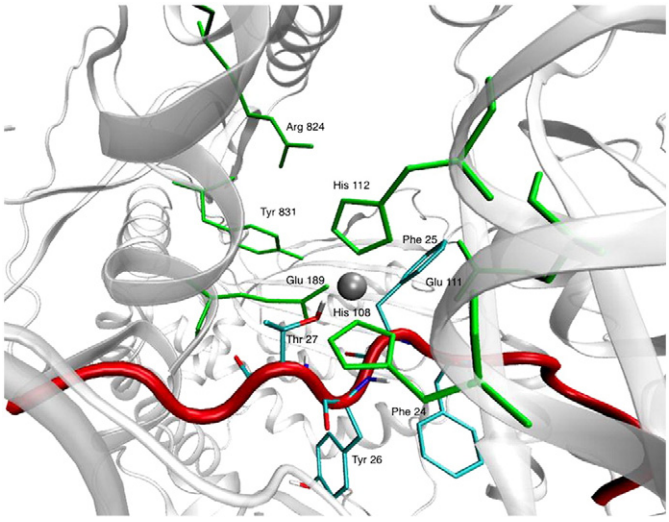

Fig. 7. Lowest energy docking structure of the IDE/B20–30 monomeric complex. The zinc coordination site faces the ^{24}PhePheTyrThr^{27} segment of B20–30. Thr27 is in close proximity to the zinc(II) ion participating in a metal–OH interaction. His108, His112, Glu111, Glu189, Tyr831 and Arg824 are shown by green sticks, and zinc(II) ion is shown by a gray sphere. The B20–30 segment is shown by sticks and a red ribbon; the IDE surrounding is shown by silver ribbons.

by a hydroxide bound to the zinc(II) ion [71] that can be stabilized by the T27 of the B20–30.

In a previous work [54] we have predicted by MD simulations that copper(I) is able to affect the hydrophobic network of the IDE binding site by a linear coordination of the two cysteines Cys812 and Cys819 which face the hydrophobic core. This interaction should alter the site shape leading to a dramatic destabilization of the active cavity and abolishing the enzymatic activity; this prediction is confirmed by present data, clearly indicating that this is a realistic mechanism. The oxidation state of the metal ion is very important in this respect, since, unlike copper(I), copper(II) brings about a much less dramatic inhibition of IDE activity through a non-competitive allosteric mechanism, which has been here elucidated, such that the IDE activity is significantly reduced but not abolished upon interaction of IDE with copper(II) (see Scheme 1). This effect is obviously metal-dependent, since the addition of zinc(II) instead of copper(II) does not lead to any inhibitory effect, actually somewhat enhancing the IDE proteolytic activity. This clarification has been possible thanks to the use of an insulin-derived peptide (i.e., B20–30) which does not bind metal ions, thus allowing a clear-cut discrimination between the metal ion effect on the enzyme and on the substrate.

4. Conclusions

Insulin is a central regulator of glucose homeostasis and its catabolism is mediated primarily by IDE in many different locations, such as the liver [72], muscle and human cerebrovascular endothelial cell cultures [73]. It is well known that impairments in insulin signaling lead to pathological conditions, such as diabetes mellitus; therefore, the possibility to enhance insulin availability by inhibiting IDE might be of the utmost therapeutic relevance [74]. However, there is a lack of a definitive study that clearly establishes within which cellular compartment insulin hydrolysis occurs [75]. IDE is primarily cytosolic but it was also found in peroxisomes [76], endosomes [77], mitochondria [78] and plasma membranes [79]; however, since neither of these compartments is believed to contain insulin, they cannot be the site of its catabolism. Moreover, it is known that metals are essential for many metabolic processes and their homeostasis is crucial in every living cell. Therefore, the alteration of metal homeostasis could turn out in cell death or severe illness as neurodegenerative disorders [25].

In this context, the investigation on the mechanism by which metal ions could modulate IDE activity toward Aβ peptides and insulin should have a great pharmaceutical impact, also because it is known that metal ions, such as copper(II) and zinc(II) induce insulin aggregation and that their imbalance is critical in DM2 pathogenesis.

Although we are perfectly aware that the reported findings have been observed with a model peptide and one could argue that our findings might not be too relevant in a biological system, we want to stress the fact that only this approach, employing a newly synthesized peptide (i.e., B20–30), which does not bind metals, allows us to determine unequivocally the very different effects of copper(II), copper(I), silver(I), aluminum(III) and zinc(II) on IDE activity; this information could not have been obtained with full size substrates (i.e., Aβ peptides and insulin) and it is of the utmost relevance for the control of IDE activity independent on the enzymatically processed substrate. The system we describe might become realistic wherever IDE is bound with metal ions in a compartment before it encounters insulin molecules in a metal-free environment. In this case, in vivo, the activity modulation of IDE by metal ions would occur toward insulin molecules in the way described above, without incurring into the discussed metal-induced insulin oligomerization issues. In this way, our findings become relevant also in a biological system.

Finally, we would like to point out that the metal concentrations used in the above described experiments mimic very well those encountered in many biological environments. Zinc(II) in the brain reaches levels up to 300 μM in the synaptic cleft of the glutaminergic neurons [24,70]; this concentration value is higher than that found for copper(II) in the same district (30 μM). In conclusion, alterations of such metal ratios might bring about severe pathological conditions, such as DM2 or AD, and the above described effect of metal ions on IDE activity could explain the link often reported between altered IDE activity and those diseases.

Acknowledgments

We thank MIUR (FIRB: RBIN04L28Y, RBRN07BMCT and RBPR05JH2P_021) and Catania University for its financial support. Dott. Chiara Damante is also gratefully acknowledged for her scientific support during the B20–30 peptide synthesis.

References

[1] W.C. Duckworth, R.G. Bennett, F.G. Hamel, Endocr. Rev. 19 (1998) 608–624.
[2] J.P.F. Bai, L.L. Chang, Pharm. Res. 12 (1995) 1171–1175.
[3] W. Farris, S. Mansourian, Y. Chang, L. Lindsley, E.A. Eckman, M.P. Frosch, C.B. Eckman, R.E. Tanzi, D.J. Selkoe, S. Guénette, Proc. Natl. Acad. Sci. U. S. A. 100 (2003) 4162–4167.
[4] W.C. Duckworth, Endocr. Rev. 9 (1988) 319–345.
[5] W.Q. Qiu, M.F. Folstein, Neurobiol. Aging 27 (2006) 190–198.
[6] M.E.-L. Blomqvist, P.A. Silburn, D.D. Buchanan, N. Andreasen, K. Blennow, N.L. Pedersen, A.J. Brookes, G.D. Mellick, J.A. Prince, Neurogenetics 5 (2004) 115–119.
[7] J.A. Luchsinger, M.X. Tang, S. Shea, R. Mayeux, Neurology 63 (2004) 1187–1192.
[8] A. Fernández-Gamba, M.C. Leal, L. Morelli, E.M. Castaño, Curr. Pharm. Des. 15 (2009) 3644–3655.
[9] J.S. Miners, P.G. Kehoe, S. Love, J. Neurosci. Methods 169 (2008) 177–181.
[10] M.C. Camberos, A.A. Perez, D.P. Udrisar, M.I. Wanderley, J.C. Cresto, Exp. Biol. Med. 226 (2001) 334–341.
[11] I.V. Kurochkin, S. Goto, FEBS Lett. 345 (1994) 33–37.
[12] A. Mukherjee, E. Song, M. Kihiko-Ehmann Jr., J.P. Goodman, J.S. Pyrek, S. Estus, L.B. Hersh, J. Neurosci. 20 (2000) 8745–8749.
[13] G. Grasso, E. Rizzarelli, G. Spoto, J. Mass Spectrom. 42 (2007) 1590–1598.
[14] G. Grasso, A.I. Bush, R. D'Agata, E. Rizzarelli, G. Spoto, Eur. Biophys. J. 38 (2009) 407–414.
[15] M.A. Leissring, A. Lu, M.M. Condron, D.B. Teplow, R.L. Stein, W. Farris, D.J. Selkoe, J. Biol. Chem. 278 (2003) 37314–37320.
[16] G. Grasso, E. Rizzarelli, G. Spoto, Biochim. Biophys. Acta 1784 (2008) 1122–1126.
[17] C. Ciaccio, G.F. Tundo, G. Grasso, G. Spoto, D. Marasco, M. Ruvo, S. Marini, E. Rizzarelli, M. Coletta, J. Mol. Biol. 385 (2009) 1556–1567.
[18] L. Morelli, R. Llovera, S.A. Gonzalez, J.L. Affranchino, F. Prelli, B. Frangine, J. Ghiso, E.M. Castaño, J. Biol. Chem. 278 (2003) 23221–23226.
[19] G. Grasso, P. Mineo, E. Rizzarelli, G. Spoto, Int. J. Mass Spectrom. 282 (2009) 50–55.

[20] V. Chesneau, K. Vekrellis, M.R. Rosner, D.J. Selkoe, Biochem. J. 351 (2000) 509–516.
[21] I.V. Kurochkin, FEBS Lett. 427 (1998) 153–156.
[22] Y. Shen, A. Joachimiak, M.R. Rosner, W.-J. Tang, Nature 443 (2006) 870–874.
[23] M. Manolopoulou, Q. Guo, E. Malito, A.B. Schilling, W.-J. Tang, J. Biol. Chem. 284 (2009) 14177–14188.
[24] D. Milardi, E. Rizzarelli, Neurodegeneration: Metallostasis and Proteostasis, Royal Society of Chemistry, 2011.
[25] N. Nelson, EMBO J. 18 (1999) 4361–4371.
[26] G. Lupidi, M. Angeletti, A.M. Eleuteri, E. Fioretti, S. Marini, M. Gioia, M. Coletta, Coord. Chem. Rev. 228 (2002) 263–269.
[27] E. Mocchegiani, R. Giacconi, M. Malavolta, Trends Mol. Med. 14 (2008) 419–428.
[28] A. Tanaka, H. Kaneto, T. Miyatsuka, K. Yamamoto, K. Yoshiuchi, Y. Yamasaki, I. Shimomura, T.A. Matsuoka, M. Matsuhisa, Endocr. J. 56 (2009) 699–706.
[29] H. Roth, M. Kirchgessner, Biol. Trace Elem. Res. 3 (1981) 13–32.
[30] W.B. Kinlaw, A.S. Levine, J.E. Morley, S.E. Silvis, C.J. McClain, Am. J. Med. 75 (1983) 273–277.
[31] P. Schott-Ohly, A. Lgssiar, H.J. Partke, M. Hassan, N. Friesen, H. Gleichmann, Exp. Biol. Med. (Maywood) 229 (2004) 1177–1185.
[32] R.A. Al-Maroof, S.S. Al-Sharbatti, Saudi Med. J. 27 (2006) 344–350.
[33] V. Beletate, R.P. El Dib, A.N. Atallah, Cochrane Database Syst. Rev. 1 (2007) CD005525.
[34] G. Falkous, J.B. Harris, D. Mantle, Clin. Chim. Acta 238 (1995) 125–135.
[35] D.S. Yang, J. McLaurin, K. Qin, D. Westaway, P.E. Fraser, Eur. J. Biochem. 267 (2000) 6692–6698.
[36] P.J. Crouch, D.J. Tew, T. Du, D.N. Nguyen, A. Caragounis, G. Filiz, R.E. Blake, I.A. Trounce, C.P.W. Soon, K. Laughton, K.A. Perez, Q.-X. Li, R.A. Cherny, C.L. Masters, K.J. Barnham, A.R. White, J. Neurochem. 108 (2009) 1198–1207.
[37] K.L. Epting, C. Vieille, J.G. Zeikus, R.M. Kelly, FEBS J. 272 (2005) 1454–1464.
[38] W.F. Li, X.X. Zhou, P. Lu, Biotechnol. Adv. 23 (2005) 271–281.
[39] C. Vieille, G.J. Zeikus, Microbiol. Mol. Biol. Rev. 65 (2001) 1–43.
[40] A.L. Pey, A. Martinez, J. Biol. Inorg. Chem. 14 (2009) 521–531.
[41] S.Z. Potter, H. Zhu, B.F. Shaw, J.A. Rodriguez, P.A. Doucette, S.H. Sohn, A. Durazo, K.F. Faull, E.B. Gralla, A.M. Nersissian, J.S. Valentine, J. Am. Chem. Soc. 129 (2007) 4575–4583.
[42] Q. Han, Y. Fu, H. Zhou, Y. He, Y. Luo, FEBS Lett. 581 (2007) 3027–3032.
[43] J.M. Hadden, A.-C. Declais, S.E.V. Phillips, D.M. Lilley, EMBO J. 21 (2002) 3505–3515.
[44] N. Selevsek, S. Rival, A. Tholey, E. Heinzle, U. Heinz, L. Hemmingsen, H.W. Adolph, J. Biol. Chem. 284 (2009) 16419–16431.
[45] S. Maric, S.M. Donnelly, M.W. Robinson, T. Skinner-Adams, K.R. Trenholme, D.L. Gardiner, J.P. Dalton, C.M. Stack, J. Lowther, Biochemistry 48 (2009) 5435–5439.
[46] M.F. Souliere, J.-P. Perreault, M. Bisaillon, Biochem. J. 420 (2009) 27–35.
[47] J. Arima, Y. Uesugi, T. Hatanaka, Biochimie 91 (2009) 568–576.
[48] B. Lai, Y. Li, A. Cao, L. Lai, Biochemistry 42 (2003) 785–791.
[49] P.A. Benkovic, C.A. Caperelli, M. de Maine, S.J. Benkovic, Proc. Natl. Acad. Sci. U. S. A. 75 (1978) 2185–2189.
[50] B. Krajewska, J. Enzyme Inhib. Med. Chem. 23 (2008) 535–542.
[51] S.C. Graham, C.S. Bond, H.C. Freeman, J.M. Guss, Biochemistry 44 (2005) 13820–13836.
[52] G. Bellomo, P.L. Nicotera, F. Travaglino, M.A. Palma, F. Mirabelli, P. Fratino, Acta Diabetol. 22 (1985) 63–69.
[53] G. Grasso, E. Rizzarelli, G. Spoto, J. Mass Spectrom. 44 (2009) 735–741.
[54] G. Grasso, A. Pietropaolo, G. Spoto, G. Pappalardo, G. Raffaella Tundo, C. Ciaccio, M. Coletta, E. Rizzarelli, Chem. Eur. J. 17 (2011) 2752–2762.
[55] C.A. Damante, K. Ősz, Z. Nagy, G. Pappalardo, G. Grasso, G. Impellizzeri, E. Rizzarelli, I. Sóvágó, Inorg. Chem. 47 (2008) 9669–9683.
[56] C.A. Damante, K. Ősz, Z. Nagy, G. Pappalardo, G. Grasso, G. Impellizzeri, E. Rizzarelli, I. Sóvágó, Inorg. Chem. 48 (2009) 10405–10415.
[57] C.A. Damante, K. Ősz, Z. Nagy, G. Grasso, G. Pappalardo, E. Rizzarelli, I. Sóvágó, Inorg. Chem. 50 (2011) 5342–5350.
[58] J. Shearer, P. Soh, Inorg. Chem. 46 (2007) 710–719.
[59] H.-C. Liang, E. Kim, C.D. Incarvito, A.L. Rheingold, K.D. Karlin, Inorg. Chem. 41 (2002) 2209–2212.
[60] V.I. Timofeev, R.N. Chuprov-Netochin, V.R. Samigina, V.V. Bezuglov, K.A. Miroshnikov, I.P. Kuranova, Acta Crystallogr. 66 (2010) 259–263.
[61] S.J. de Vries, M. van Dijk, A.M.J.J. Bonvin, Nat. Protoc. 5 (2010) 883–897.
[62] P.T. Grant, T.L. Coombs, B.H. Frank, Biochem. J. 126 (1972) 433–440.
[63] R. Sreekanth, V. Pattabhi, S.S. Rajan, Int. J. Biol. Macromol. 44 (2009) 29–36.
[64] G. Grasso, Mass Spectrom. Rev. 30 (2011) 347–365.
[65] I. Bertini, H.B. Gray, E.I. Stiefel, J.S. Valentine, Biological inorganic chemistry, Structure and Reactivity, 2007.
[66] A.C. Miu, O.J. Benga, J. Alzheimers Dis. 10 (2006) 179–201.
[67] D. Drago, S. Bolognin, P. Zatta, Curr. Alzheimer Res. 5 (2008) 500–507.
[68] D.L. Huffman, T.V. O'Halloran, Annu. Rev. Biochem. 70 (2001) 677–701.
[69] E. Malito, L.A. Ralat, M. Manolopoulou, J.L. Tsay, N.L. Wadlington, W.-J. Tang, Biochemistry 47 (2008) 12822–12834.
[70] D.W. Christianson, D.W. Cox, Annu. Rev. Biochem. 68 (1999) 33–57.
[71] O. Amata, T. Marino, N. Russo, M. Toscano, J. Am. Chem. Soc. 131 (2009) 14804–14811.
[72] H. Akiyama, K. Shii, K. Yokono, K. Yonezawa, S. Sato, K. Watanabe, S. Baba, Biochem. Biophys. Res. Commun. 155 (1988) 914–922.
[73] W. Gao, P.B. Eisenhauer, K. Conn, J.A. Lynch, J.M. Wells, M.D. Ullman, A. McKee, H.S. Thatte, R.E. Fine, Neurosci. Lett. 371 (2004) 6–11.
[74] M.A. Leissring, E. Malito, S. Hedouin, L. Reinstatler, T. Sahara, S.O. Abdul-Hay, S. Choudhry, G.M. Maharvi, A.H. Fauq, M. Huzarska, P.S. May, S. Choi, T.P. Logan, B.E. Turk, L.C. Cantley, M. Manolopoulou, W.-J. Tang, R.L. Stein, G.D. Cuny, D.J. Selkoe, PLoS One 5 (2010) e10504.
[75] L.B. Hersh, Cell. Mol. Life Sci. 63 (2006) 2432–2434.
[76] F. Authier, B.I. Posner, J.J. Bergeron, Clin. Invest. Med. 19 (1996) 149–160.
[77] F.G. Hamel, M.J. Mahoney, W.C. Duckworth, Diabetes 40 (1991) 436–443.
[78] W. Farris, M.A. Leissring, M.L. Hemming, A.Y. Chang, D.J. Selkoe, Biochemistry 44 (2005) 6513–6525.
[79] E.L. Que, D.W. Domaille, C.J. Chang, Chem. Rev. 108 (2008) 1517–1549.